Journal of Wind Engineering and Industrial Aerodynamics, 15 (1983) 317–327
Elsevier Science Publishers B.V., Amsterdam — Printed in The Netherlands

MINIMUM INDUCED LOSS WINDMILLS AND PROPELLERS

E. Eugene Larrabee and Susan E. French
Department of Aero- and Astronautics, M.I.T., Cambridge, MA

SUMMARY

Horizontal axis wind turbines can be designed advantageously to utilize minimum induced loss radial loading, exactly inverse to that of high efficiency airplane propellers, as described by Betz, Prandtl, (1919) and Goldstein (1929). Benefits include reduced tower load and increased wind energy for windmills downstream in an array. At M.I.T. the authors have developed a rotor design and analysis code, HELICE, which exploits analytic simplifications possible with near minimum induced loss loading. Earlier versions have been used to design propellers for human powered airplanes (1979) and windmills (1980). Algorithms and exmples are given.

1. MINIMUM INDUCED LOSS WINGS AND ROTORS; BACKGROUND

The idea of "minimum induced loss" comes from Prandtl and his circle at Goettingen who noted the analogy between the magnetic field induced by an array of conductors and the velocity field of a geometrically similar array of line vortices, both described by the Biot-Savart law. By 1916 they had discovered that a spanwise elliptic distribution of lift (and bound vorticity) led to a spanwise uniform "downwash" of the trailing vortex sheet and minimum kinetic energy of the wing velocity field for a specified lift, wing span, and airspeed. By 1919 Betz [1] had established a similar rule for the motion of the helicoidal trailing vortex sheets shed by a propeller (unfortunately called the "rigid wake condition" by Betz himself), and Prandtl had devised an appropriate analytic solution for the corresponding radial distribution of bound vorticity which would minimize the kinetic energy of a propeller velocity field for a specified thrust, propeller diameter, shaft speed, airspeed, and number of blades. As a post doctoral fellow at Goettingen, Sydney Goldstein refined the Betz-Prandtl theory of propellers, and publication of his paper by the Royal Society [2] in 1929 brought it to the attention of the English speaking aeronautical community. Glauert wrote an admirable review of this theory in 1934 [3] shortly before his untimely death.

In 1969 I began examining the theory to develop inexpensive propeller design and analysis techniques for amateur airplane constructors, giving algorithms [4] in 1979 which were used to design propellers of high efficiency for the Gossamer Albatross [5] and Chrysalis [6] human powered airplanes. Under my direction my

0167-6105/83/$03.00

coauthor wrote several FORTRAN codes named HELICE which incorporated these algorithms and were adapted to a small Digital Equipment Corporation PDP-11/45 computer using the RT-11 operating system. I then realized that HELICE would do windmills as well as propellers, and that the minimum induced loss loading feature of the design subroutine would improve the "inverse propeller" or "ram air turbine" efficiency of the rotor. Recently, it has been used to design three windmills: a small one for research, a large one for power generation, and the one seen in Fig. 1.

Fig. 1. "La Molina Migliora", a windmill designed for Robert Migliori, an architect in Portland, Oregon. It is used to cancel domestic power consumption on the average. 6.4 m diameter, rated at 7.46 kW shaft power at 204 rpm in a 10.7 ms^{-1} wind.

The HELICE rotor design and analysis code is based on the following ideas, which will be described in turn:

1) a reinterpretation of Betz's rigid wake condition;
2) the essential correctness of Prandtl's analytic radial circulation distribution;

3) the use of simple loading integrals to determine the slipstream "displacement" velocity and the corresponding rotor geometry,
4) an approximate algorithm for induced velocities at the rotor lifting lines consistent with Prandtl's loading from (2) above; and
5) a simple analytic representation of blade section aerodynamics for angles of attack from -90° to +90°.

2. BETZ'S RIGID WAKE CONDITION REINTERPRETED

Betz said that helicoidal vortex sheets shed by a minimum induced loss propeller should move as rigid bodies, translating axially with a certain "displacement" velocity, or rotating about the propeller shaft axis with a certain angular velocity. Actually trailing vortex sheets move locally perpendicular to themselves. If the local helix angle is ϕ(Fig.2) and the radially constant displacement velocity is v', the appearance of rigid body axial motion will be given if the local sheet velocity is $v'\cos\phi$. Corresponding axial and swirl velocities of the "developed" vortex sheet are $v'\cos^2\phi$ and $v'\cos\phi\sin\phi$, respectively, inconsistent with rigid body motion. Induced velocities at the rotor lifting lines are just half these values, as in wing theory.

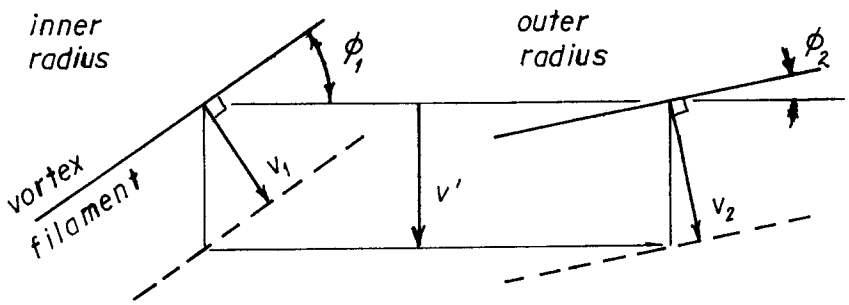

Fig.2. Betz's "rigid wake condition" for minimum loss reinterpreted. Local sheet velocity = $v'\cos\phi$, v' = displacement velocity.

3. PRANDTL'S APPROXIMATE RADIAL CIRCULATION DISTRIBUTION

If the rotor has B blades and is "lightly loaded", the bound circulation Γ on each blade at radius r is given by Stokes' law,

$$B\Gamma = 2\pi r \cdot \bar{v}_{swirl} \qquad (1)$$

where $\bar{v}_{swirl}$ is the average swirl velocity in the developed slipstream at radius r. The average swirl velocity is a fraction F of the local swirl velocity of the vortex sheets given above. Since the rotor is "lightly loaded"

$$\cos\phi \cong x/\sqrt{x^2 + 1} \; ; \quad x \equiv \Omega r/V, \tag{2}$$

$$\sin\phi \cong 1/\sqrt{x^2 + 1} \tag{3}$$

Prandtl approximated F with a planar flow result for the average velocity of fluid entrained by an infinite array of semi-infinite plates moving perpendicular to themselves:

$$F = \frac{\text{average fluid velocity}}{\text{plate velocity}} = (2/\pi)\arccos\left(\exp(-f)\right) \tag{4}$$

$$f = \pi\left(\frac{\text{edge distance}}{\text{plate spacing}}\right) = (B/2)\left(\sqrt{\lambda^2 + 1}\,/\lambda\right)(1 - r/R) \tag{5}$$

The expression for f corresponds to rotor wake geometry, where $\lambda \equiv V/\Omega R$, with R the tip radius. I chose the symbol G for the corresponding dimensionless circulation function in honor of Goldstein:

$$G \equiv \frac{B\Omega\Gamma}{2\pi V v'} \cong \frac{Fx^2}{x^2 + 1} \; ; \quad \text{(Prandtl's approximation)} \tag{6}$$

Figure 3 compares Goldstein's painfully calculated "exact" circulation functions for minimum induced loss circulation distribution with Prandtl's (eq.6) approximates ones; Prandtl's are accurate enough whenever outer edge vortex sheet spacing is less than rotor tip radius. The quantity G also may be interpreted as the ratio of average axial velocity in the developed slipstream to displacement velocity v'.

4. DETERMINATION OF THE DISPLACEMENT VELOCITY AND ROTOR GEOMETRY

Using light loading approximations again, the thrust coefficient $T_c \equiv 2T/\rho V^2\pi R^2$ and power coefficient $P_c \equiv 2P/\rho V^3\pi R^2$ can be written in terms of displacement velocity ratio, $\zeta \equiv v'/V$, and integrals which correspond to minimum induced loss loading and account for blade element profile drag:

$$T_c = I_1\zeta - I_2\zeta^2 \tag{7}$$

$$P_c = J_1\zeta + J_2\zeta^2 \tag{8}$$

$$I_1 = 4\int_o^1 G\left\{1 - \frac{D/L}{x}\right\}\xi d\xi \; ; \quad \xi = r/R \tag{9}$$

$$I_2 = 2\int_o^1 G\left\{1 - \frac{D/L}{x}\right\}\left\{1/(x^2 + 1)\right\}\xi d\xi \tag{10}$$

$$J_1 = 4\int_o^1 G\left\{1 + (D/L)x\right\}\xi d\xi \tag{11}$$

$$J_2 = 2 \int_0^1 G\{1 + (D/L)x\}\{x^2/(x^2 + 1)\}\ \xi d\xi \tag{12}$$

Thus, if disc loading (P_c), wake geometry ($B,\lambda \rightarrow G$), and radial variation of blade element $D/L = c_d/c_\ell$ are known, displacement velocity ratio is

$$\zeta = (J_1/2J_2)\left[\sqrt{1 + (4P_c J_2/J_1^2)} - 1\right]^* \tag{13}$$

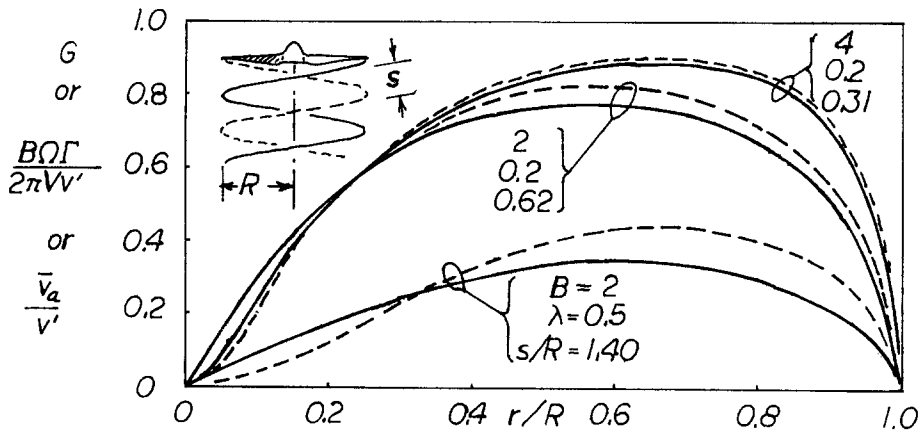

Fig. 3. Prandtl (dashed lines) and Goldstein (solid lines) circulation distributions for minimum induced loss compared.

Then the helix angle of the blade element flow is given by

$$\phi = \arctan\left|\frac{\lambda}{\xi}\left(1 + \frac{\zeta}{2}\right)\right| \tag{14}$$

and the blade element velocity ratio is

$$W/V = \sqrt{x^2 + 1 - \left(\frac{\zeta}{2}\cos\phi\right)^2} \tag{15}$$

The blade angle of the corresponding minimum induced loss rotor is given by

$$\beta = \phi + \alpha_D \tag{16}$$

where α_D is the blade element design angle of attack in planar flow corresponding to D/L. Finally, the blade chord is given by

---

*Compare $\alpha_{\text{induced (radians)}} = \dfrac{2C_L}{\pi(b^2/S)}$ for an elliptically loaded wing.

$$c/R = (4\pi\lambda/B)(G/(W/V))(\zeta/c_\ell) \tag{17}$$

where c_ℓ is the blade element lift coefficient at α_D . It will be appreciated that T_c, P_c, D/L, ζ, and c_ℓ are all positive for propellers and negative for windmills. In HELICE the integrals are numericaly evaluated by Simpson's rule for r/R = 0, 0.1, 0.2... 1.0.

5. AN APPROXIMATE ALGORITHM FOR INDUCED ANGLE OF ATTACK

In the case of rotors of arbitrary geometry, or a minimum induced loss rotor operating off its design point, displacement velocity is no longer radially uniform and induced velocity at the blade elements is no longer 1/2 v'cosϕ . Instead the induced angle of attack may be approximated by

$$\alpha_{induced}(\text{radians}) = \frac{1}{4}\left(\frac{\sigma\sqrt{x^2+1}}{F}\right) c_\ell \tag{18}$$

where $\sigma = Bc/2\pi r = (B/2\pi)(c/R)/(r/R)$ is the local rotor solidity. To be strictly consistent with the minimum induced loss rotor geometry determination procedure just given, this should be written

$$\alpha_{induced} = \arcsin\left[\frac{1}{4}\left(\frac{\sigma\sqrt{x^2+1}}{F}\right)\left\{\frac{\sqrt{(x^2+1)\{x^2+(1+\frac{\zeta}{2})^2\}-(\frac{\zeta}{2}x)^2}}{\{x^2+(1+\frac{\zeta}{2})^2\}}\right\} c_\ell\right] \tag{18a}$$

which is computationally inconvenient. The error is small if $|\zeta|$ is small.

Alternatively the axial and swirl components of the induced velocity can be calculated by a radially graded momentum theory as suggested by Glauert, but written down incorrectly in [3], which is also more or less consistent with minimum induced loss loading:

$$\frac{a}{1+a} = \frac{1}{4}\frac{\sigma(c_\ell\cos\phi - c_d\sin\phi)}{F\sin^2\phi} \tag{19}$$

$$\frac{a'}{1-a'} = \frac{1}{4}\frac{\sigma(c_\ell\sin\phi + c_d\cos\phi)}{F\sin\phi\cos\phi} \tag{20}$$

here aV and a'Ωr are the axial and swirl components of the induced velocity. I have recommended the procedure [4], although I find it less convenient computationally, and less consistent with the minimum induced loss rotor geometry determination subroutine in the previous section, than a procedure based on equation 18.

6. BLADE SECTION AERODYNAMICS

The blade section aerodynamic properties in HELICE are taken to be analytic functions of the blade element angle of attack in planar flow for $(-90^0<\alpha<+90^0)$:

$$c_\ell = c_{\ell_1} \cos\alpha/\cos\alpha_1 \qquad \text{negative stall range} \qquad (21)$$

$$c_d = |\sin\alpha| \qquad \alpha<\alpha_1 \qquad (22)$$

$$c_\ell = c_{\ell_1} + \left\{\frac{c_{\ell_2} - c_{\ell_1}}{\alpha_2 - \alpha_1}\right\}(\alpha - \alpha_1) \qquad \text{unstalled range} \qquad (23)$$

$$c_d = c_{d_3} + \frac{dcd}{d(\alpha^2)}(\alpha - \alpha_3)^2 \qquad \alpha_1 \leq \alpha \leq \alpha_2 \qquad (24)$$

$$c_\ell = c_{\ell_2} \cos\alpha/\cos\alpha_2 \qquad \text{positive stall range} \qquad (25)$$

$$c_d = |\sin\alpha| \qquad \alpha>\alpha_2 \qquad (21) \text{ repeated}$$

Default values of blade section parameters in HELICE corresponding to NACA 4412 or 4415 airfoils at moderate Reynolds number are in Table 1.

TABLE 1
HELICE blade section default values

parameter	propeller	windmill
c_{ℓ_1}	-0.8	-1.2
α_1	-12.0°	-8.0°
c_{ℓ_2}	+1.2	+0.8
α_2	+8.0°	+12.0°
c_{d_3}	0.008	0.008
α_3	-2.0°	+2.0°
$dc_d/d(\alpha^2)$	0.00025/(deg^2)	0.00025/(deg^2)

So windmill values are propeller values "turned over"; i.e., the blade cambered faces are downstream. HELICE users introduce these values, or any of their choosing, at each of nine radial stations for r/R = 0.1, 0.2, 0.3,...0.9.

7. EXPERIMENTAL VALIDATION OF HELICE

For propellers, HELICE has been validated by the Chrysalis and Gossamer Albatross human powered airplanes; for windmills, HELICE design and performance routines have been validated by tests on the windmills cited. Figure 4 compares HELICE predictions of windmill performance with high quality wind tunnel data obtained by de Vries and coworkers at the NLR [7]. Like other lifting line analysis methods, HELICE can be adjusted readily to give a wide range of "reasonable" answers. Table 2 gives HELICE parameters used for Fig. 4.

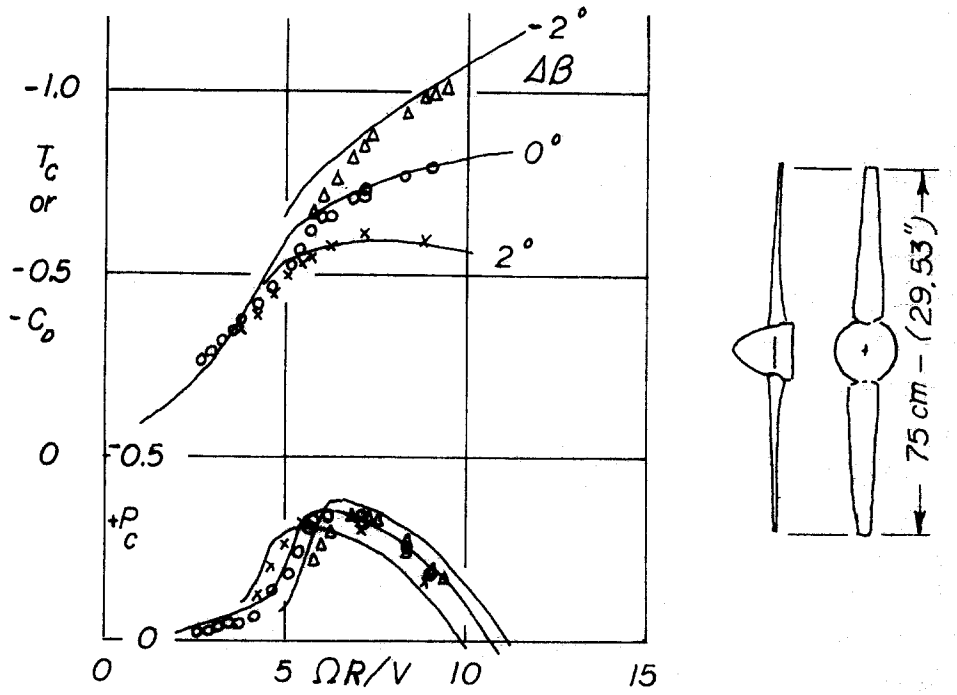

Fig 4. Validation of HELICE with de Vries' experimental data [7]. See Table 2 for HELICE parameters.

TABLE 2

HELICE parameters for NLR research windmill 2 blades-NACA 0012 airfoil sections.

parameters	0.1*	0.2	0.3	0.4	0.5	0.6	0.7	0.8	0.9
c_{ℓ_1}	-1.26	-1.24	-1.22	-1.20	-1.18	-1.16	-1.14	-1.12	-1.10
α_1^0	-11.48	-11.42	-11.36	-11.30	-11.24	-11.18	-11.12	-11.06	-11.00
c_{ℓ_2}	1.26	1.24	1.22	1.20	1.18	1.16	1.14	1.12	1.10
α_2^0	11.48	11.42	11.36	11.30	11.24	11.18	11.12	11.06	11.00
c_{d_3}	0.010	0.014	0.018	0.022	0.026	0.030	0.034	0.038	0.042
α_3^0	0	0	0	0	0	0	0	0	0
$\frac{dc_d}{d(\alpha^2)} \times 10^{-3}$	0.24	0.25	0.26	0.27	0.28	0.29	0.30	0.31	0.32
c/R†	0.21	0.192	0.174	0.156	0.138	0.120	0.102	0.084	0.066
β^0†	41.761	19.940	11.921	7.664	4.006	3.154	1.600	0.759	-0.068

*The r/R = 0.1 station does not exist; it is inside the spinner. The values chosen give a benign radial loading whose radial integrals agree with the actual loading integrals.
†actual geometry

The elevated values of c_{d_3} are required to reduce predicted rotor power to experimental values. Presumably this models the excessive radial growth of blade boundary layer momentum thickness caused by heavy centrifugal stresses associated with high wind speeds (V = 35 ms^{-1}) and shaft speeds (~5000 rpm) needed to maintain satisfactory blade chord Reynolds numbers with a 75 cm diameter rotor.

8. TYPICAL MINIMUM INDUCED LOSS WINDMILL DESIGN AND PERFORMANCE

Figure 5 gives the geometry and performance of a typical minimum induced loss windmill with design characteristics summarized in Table 3:

TABLE 3

Design Point Input for HELICE windmill design subroutine 2 blades, default aerodynamics (NACA 4415 airfoils)

-77,932 watts shafts power (76 kW intended)
66.667 rotor rpm corresponds to 1860 generator rpm
10 ms^{-1} (22.37 mph) rated power wind speed
10 m rotor radius (65.62 ft. diameter)
1.2 kg/m^3 air density (cf. 1.225 kg/m^3 @ 760 mm Hg and 15°C)
design blade angles of attack for r/R = 0.1, 0.2, 0.3 ...0.9
-4.0°, -5.0°, -5.75°, -6.0°, -6.1°, -6.2°, -6.3°, -6.4°, -6.5°

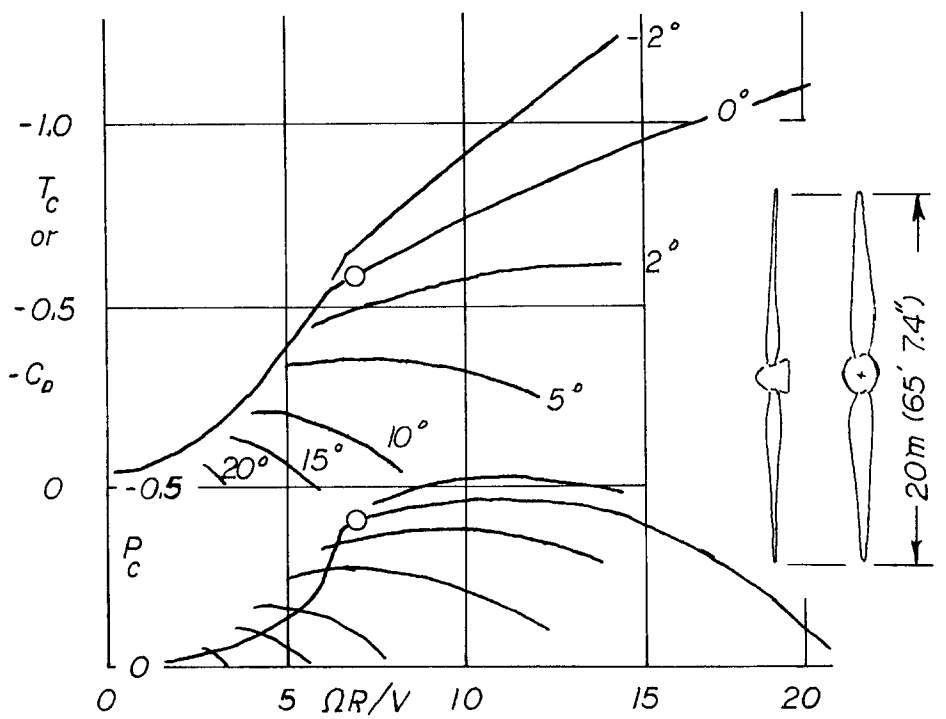

Fig. 5. HELICE windmill design and performance. Circles indicate design point; for design parameters see Table 3.

The design point performance (circles, Fig. 5) is calculated to be T_c = -0.5757($-T_c$ = rotor drag coefficient) and P_c = -0.4028, or 40.28% of the kinetic energy of undisturbed stream flow through the rotor disc area in unit time, at a tip speed ratio of 6.981. By decreasing blade angles 2° and increasing tip speed ratio to 11, P_c becomes -0.5219 (the actuator disc limit is -0.5926) at the expense of a 70% increase in rotor drag (T_c = -0.9816). The designer chooses the operating point.

Figure 6 shows stall mode and blade angle governing of this windmill driving an asynchronous generator (induction motor) connected to a 60 Hz grid. The cut-in speed of 4.2 ms^{-1} corresponds to the mechanical power loss for 1800 generator rpm. The rotor may be run at design blade angles from below cut-in speed to a wind speed of 24 ms^{-1}, when the output of the stalled rotor drives electrical output of the generator to 150% rating, where coil winding temperatures may be critical. At higher speeds it must be shut down. A windmill of this size might well use blade angle governing to limit power to the rated value for all wind speeds greater than 10 ms^{-1}. Tower loads will be greatly reduced, and the shut down speed will not exist if enough governing blade angle range has been provided. HELICE also will predict torque of an almost stopped rotor (tip speed ratio = 0.05), showing that about 85° blade angle increase is needed to stop the rotor without a brake.

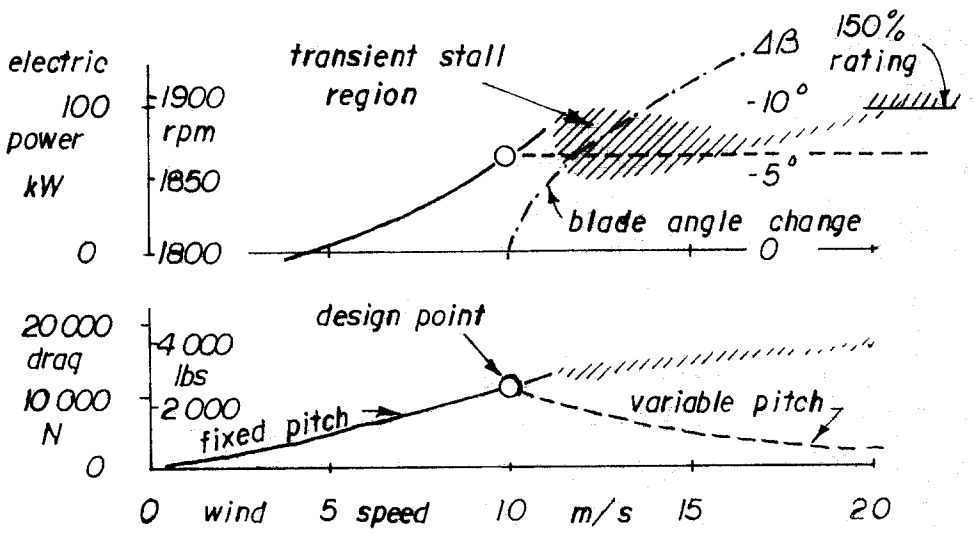

Fig. 6. Fixed pitch (showing stall governing) and variable pitch operation of the windmill of Fig. 5 with generator load.

REFERENCES

1 R.T. Jones (compiled by), Classical aerodynamic theory. NASA Reference Publication 1050 (1979); includes NACA Technical Report No. 116 "Applications of modern hydrodynamics to aeronautics" by L. Prandtl (pps. 1-55 of the Compilation). This document, written by Prandtl in German about 1921 and published in 1923 is one of the few good English translations produced by the NACA.

2 S. Goldstein, On the vortex theory of screw propellers, Proceedings of the Royal Society, A, Vol. 123 (1929).

3 H. Glauert, Airplane propellers, Div. L. Vol. IV of "Aerodynamic Theory" edited by Durand; Springer-Verlag 1935; also Dover photo offset reprint.

4 E.E. Larrabee, Design of propellers for motorsoarers, "Science and Technology of Low Speed and Motorless Flight", NASA Conference Publication 2085, Part 1, (1979) 285-303.

5 M. Grosser, Gossamer Odyssey - the triumph of human-powered flight, Houghton Mifflin Company, Boston, 1981.

6 Janes All the World's Aircraft, (1981-82) 413-414. Also "Soaring" magazine, Vol. 43, No. 10, (1979) 36-41.

7 O. de Vries, Wind tunnel tests on a model of a two-bladed horizontal axis wind turbine and evaluation of an aerodynamic performance calculation method, NLR TR 79071 L National-Lucht-en Ruimtevaartlaboratorium, Amsterdam (1979).